Cancer Chemother Pharmacol (2012) 69:173–183
DOI 10.1007/s00280-011-1681-1

ORIGINAL ARTICLE

Preclinical anti-angiogenesis and anti-tumor activity of SIM010603, an oral, multi-targets receptor tyrosine kinases inhibitor

Dongchun Wang · Feng Tang · Sen Wang · Zhenzhou Jiang · Luyong Zhang

Received: 9 March 2011 / Accepted: 11 May 2011 / Published online: 3 June 2011

Abstract
Objective SIM010603 is a structurally novel, oral, multi-targeted receptor tyrosine kinase inhibitor. This study investigated the anti-angiogenic and anti-tumor effects of SIM010603.
Methods A radiometric protein kinase assay was used for measuring the kinase activity of the 32 protein kinases. Receptor phosphorylation was determined by enzyme-linked immunosorbent assay (ELISA). Cell proliferation was measured by 3-(4, 5-dimethylthiazol-2-yl)-2,5-diphenyl tetrazolium bromide (MTT) assay. Cell chemotaxis was evaluated by modified Boyden chamber assay. Effect of SIM010603 on angiogenesis was examined by mouse cornea angiogenesis assay. Effect of SIM010603 on xenografts was assessed by tumor growth delay. Effects of SIM010603 on tumor microvascular density (MVD), recruitment of pericytes, and pericyte encapsulation of tumor vessels were analyzed by immunofluorescent staining technique.
Results SIM010603 inhibited stem cell factor receptor (Kit), vascular endothelial growth factor receptor-2 (VEGFR-2), platelet-derived growth factor receptor-β (PDGFR-β), glial cell line-derived neurotrophic factor receptor (Rearranged during Transfection; RET), and Fms-like tyrosine kinase-3 (FLT3) with IC_{50} values between 5.0 and 68.1 nmol/l. SIM010603 inhibited the phosphorylation of PDGFR-β and VEGFR-2. Moreover, SIM010603 inhibited endothelial cell proliferation, endothelial cells chemotaxis, and corneal angiogenesis. Although SIM010603 exhibited lower activity in regard to proliferation of NCI-H460, MDA-MB-435, and T241-VEGF-A cells ($IC_{50} > 1$ μmol/l), SIM010603 inhibited tumor growth in these xenograft tumor growth models. SIM010603 reduced tumor MVD in T241-VEGF-A tumor xenograft models and decreased positive signals of CD31, NG2 in MDA-MB-435, and LLC-SW-44 xenograft tumor models.
Conclusions These results support the clinical assessment of SIM010603 as a therapeutic agent for cancer.

Keywords SIM010603 · Receptor tyrosine kinases · Anti-VEGFR · Anti-PDGFR · Angiogenesis

Electronic supplementary material The online version of this article (doi:10.1007/s00280-011-1681-1) contains supplementary material, which is available to authorized users.

D. Wang · Z. Jiang (✉) · L. Zhang (✉)
Jiangsu Center for Drug Screening, China Pharmaceutical University, 24 Tong Jia Xiang, Nanjing 210009, China
e-mail: jiangcpu@yahoo.com.cn

L. Zhang
e-mail: drugscreen@126.com

Z. Jiang · L. Zhang
Key Laboratory of Drug Quality Control and Pharmacovigilance, China Pharmaceutical University, Ministry of Education, Nanjing 210009, China

L. Zhang
JiangSu Center for Pharmacodynamics Research and Evaluation, China Pharmaceutical University, Nanjing 210009, China

D. Wang · F. Tang · S. Wang
Jiangsu Simcere Pharmaceutical R&D Co., Ltd., Nanjing 210042, China

Introduction

Conventional chemotherapy designed to influence or abolish the ability of cancer cells to replicate does not discriminate effectively between rapidly dividing normal cells and tumor cells, thus leading to several toxic side effects. In contrast, interfering with molecular targets that have a role in tumor growth or progression (i.e., targeted

therapies) is expected to target tumor cells specifically, thus allowing for strong anti-cancer effects and minimal host toxicity. Much enthusiasm has been generated about targeted therapies in recent years, and a number of such target-based anti-cancer therapies are now successfully used in routine clinical practice [1–3].

There are multiple types of targeted therapies available, including monoclonal antibodies, inhibitors of tyrosine kinases, and anti-sense inhibitors of growth factor receptors. Receptor tyrosine kinases (RTKs) are especially important target because they play an important role in the modulation of growth factor signaling [4, 5]. In the past, major efforts were aimed at developing highly specific inhibitors to act on single RTK. Imatinib mesylate was the first RTK inhibitor developed against bcr-abl for chronic myeloid leukemia [6]. Later, two small RTK inhibitors, Erlotinib and Gefitinib, were developed against epidermal growth factor receptor (EGFR). However, most tumors do not respond to single RTK inhibition. Due to secondary mutations [7–10] and activation of alternative RTK pathways, tumors that are treated with single-targeted RTK inhibitors rapidly develop drug resistance. Currently, there is a general agreement that molecules interfering simultaneously with multiple RTKs might be more effective than single-target agents. With the FDA approval of Sorafenib- and Sunitinib-targeting vascular endothelial growth factor receptor-2 (VEGFR-2, also known as KDR), platelet-derived growth factor receptor-β (PDGFR-β), Fms-like tyrosine kinase-3 (FLT3), and stem cell factor receptor (Kit), a different scenario is emerging, where a new generation of anti-cancer drugs that able to inhibit more than one pathway will probably play a major role [11, 12].

SIM010603 is a novel, oral, multi-targeted RTK inhibitor of Kit, VEGFR, PDGFR-β, RET, and FLT3. In the present study, we described the RTK inhibitory, anti-tumor, and anti-angiogenic ability of SIM010603 in a preclinical setting.

Materials and methods

Compounds

SIM010603 (Fig. 1) was synthesized at Jiangsu Simcere Pharmaceutical R&D Co., Ltd. It has the molecular formula $C_{24}H_{29}FN_4O_2$, and its chemical name is (Z)-N-(2-(diethylamino)ethyl)-2-methyl-7-(1,2-dihydro-5-fluoro-2-oxo-3H-indol-3-ylidene)-4,5,6,7-tetrahydro-1H-indole-3-carboxamide.

Cell lines

Murine fibrosarcoma T241 cells over-expressing VEGF-A and green fluorescent protein (T241-VEGF) [13, 14] and porcine aorta endothelial cell over-expressing KDR

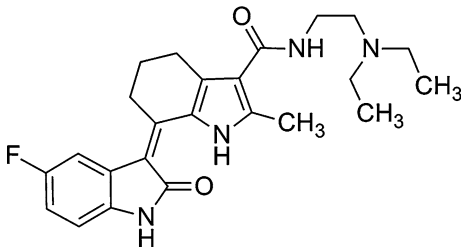

Fig. 1 Chemical structure of SIM010603

(PAE/KDR) cells were kindly provided by Dr. Yihai Cao (Ludwig Institute for Cancer Research, Uppsala, Sweden). Cells were, respectively, cultured in DMEM and Hanks' F12 medium supplemented with 10% fetal bovine serum and antibiotics. Human umbilical vein endothelial cells (HUVECs) were obtained from ScienCell Research Laboratories and were cultured in ECM medium supplemented with 5% fetal bovine serum, 1% ECGS, and antibiotics. NIH-3T3 (murine fibroblasts) and MDA-MB-435 cell lines were obtained from Shanghai Institute of Biochemistry and Cell Biology. Carcinoma cell lines (HT-29, HepG2, A549, NCI-H460, LLC-SW44, and BXPC-3) were obtained from American Type Culture Collection (ATCC) and propagated by standard tissue culture procedures in the medium suggested by the supplier.

Animals

C57BL/6 mice were obtained from Department of Microbiology, Tumor, and Cell Biology, Karolinska Institute. All animal studies were reviewed and approved by the animal care and use committees of the local animal board. BALB/c nude female mice were obtained from Shanghai SLAC Laboratory Animals Co., Ltd. (China) and housed in specific pathogen-free conditions.

Kinase assays

A radiometric protein kinase assay was used for measuring the kinase activity of the 32 protein kinases [15]. All kinase assays were performed in 96-well FlashPlates^{TM} from Perkin Elmer (Boston, MA, USA) in a final volume of 50 µl according to the following assay reaction recipe: 20 µl of assay buffer, 15 µl of [γ-^{33}P]-ATP solution, 10 µl of enzyme/substrate mixture, 5 µl of test sample (various concentrations of SIM010603 or assay buffer). The reaction mixture was incubated at 30°C for 80 min. The reaction was stopped with 50 µl of 2% (v/v) H_3PO_4, and plates were aspirated and washed two times with 200 µl 0.9% (w/v) NaCl. Incorporation of ^{33}Pi (counting of "cpm") was determined with a microplate scintillation counter (Microbeta, Wallac). IC_{50} values were calculated using

Prism 4.03 for Windows (Graphpad, San Diego, California, USA).

Receptor phosphorylation assay

Receptor phosphorylation was assessed using a sandwich enzyme-linked immunosorbent assay (ELISA) technique [16]. NIH-3T3 cells stimulated with PDGF-BB (Peprotech) were used to quantify inhibition of PDGFR-β phosphorylation, and HUVECs stimulated with $VEGF_{165}$ (Peprotech) were used to quantify inhibition of VEGFR-2 phosphorylation. Cells were seeded at 7×10^5 cells/ml in 300 µl growth medium per well in 24-well plates. After 10 h, the growth medium was replaced with 200 µl serum-depleted medium overnight. The compound was diluted in 100% dimethyl sulfoxide (DMSO), added to the cells at a final DMSO concentration of 0.1% v/v, and incubated at 37°C for 1 h. Cells were stimulated with the appropriate ligands (30 ng/ml PDGF-BB or 40 ng/ml $VEGF_{165}$) and incubated for an additional 6 min. Un-stimulated cells were used as blank and untreated but stimulated cells were used as control. The medium was removed, and the cells were washed once with PBS and then lysed with 250 µl lysis buffer [RIPA Lysis Buffer (Strong), Beyotime Institute of Biotechnology]. The diluted cell lysates were mixed thoroughly, and 100 µl of supernatant was transferred to the ELISA capture plate and incubated at 37°C for 2 h with agitation. ELISA capture plates were prepared by coating 96-well plates with 100 µl/well of 2 µg/ml goat anti-mouse PDGFR-β antibody (AF1042, RnD) or mouse anti-human VEGFR-2 antibody (AF357, RnD) overnight at 4°C. At the end of the 2-h incubation, the plates were washed (PBS, 0.1% Tween 20) before incubation with anti-phosphotyrosine antibody (Upstate, clone 4G10, diluted in PBS, 0.05% Tween 20) at 1:2,000 for 1 h at 37°C with agitation. The plates were washed again and then incubated with HRP goat anti-mouse IgG (BA1050, Boster) at 1:3,000 for 1 h at 37°C with agitation. The plates were washed a final time and then incubated with tetramethylbenzidine (Thermo) and evaluated. IC_{50} values were calculated as percent inhibition of control.

Cell proliferation assay

A 72-h cell proliferation assay was used. HUVECs were plated into 96-well plates at 3,000 cells per well and incubated with 1% serum medium for 24 h. Cells were treated with increasing concentrations of SIM010603 for 72 h at 37°C. Then, 40 ng/ml $VEGF_{165}$ (Peprotech) was added and incubated for 72 h. NIH-3T3 cells were plated into 96-well plates at 2,000 cells per well and incubated with 0.5% serum medium for 24 h. Cells were treated with increasing concentrations of SIM010603 for 1 h at 37°C. Then, the appropriate stimulate factor (30 ng/m PDGF-BB) was added and incubated for 72 h. Un-stimulated cells were used as blank and untreated, but stimulated cells were used as control. For carcinoma cell lines, 2,000 cells per well were plated overnight in full growth medium. The drug was added to the cells in full growth medium and incubated for 72 h. The effects on proliferation were determined by addition of 5 mg/ml MTT (Sigma), incubation for 4 h at 37°C in a CO_2 incubator, and analysis in an Infinite 200 Microplate Reader (Tecan). For $VEGF_{165}$- and PDGF-BB-stimulated growth, unstimulated cells were used as blank and untreated but stimulated cells were used as control. IC_{50} values were determined by nonlinear regression analysis of the concentration response data.

Chemotaxis assay

The effect of SIM010603 on $VEGF_{165}$-induced PAE/VEGFR-2 cell chemotaxis was assayed using a modified Boyden chamber technique [17, 18]. Briefly, the ability of VEGFR-2-expressing PAE cells to migrate through a micropore nitrocellulose filter (8 µm thick, 8 µm pores) was measured as a criterion for chemotactic stimuli. Approximately 40,000 cells were seeded in each upper chamber, and the cells were allowed to adhere for 1 h. Cells were then treated for 1.5 h by adding 100 µl of twofold concentrated drug solution prepared in serum-free medium into the upper chamber and 600 µl of the drug solution into the lower chamber. Migration was initiated by adding $VEGF_{165}$ (40 ng/ml) to the lower chamber. Unstimulated cells were used as blank and untreated, but stimulated cells were used as control. After 4 h incubation at 37°C, cells attached to the filter were fixed in methanol and stained with Giemsa solution. Quadruplicates of each sample were used, and all experiments were performed twice. The cells that had migrated through the filter were counted using a light microscope and plotted as numbers of migrating cells per optic field (32×).

Corneal angiogenesis assay

The mouse corneal assay was performed according to procedures described previously [19]. Corneal micropockets were created with a modified von Graefe cataract knife in both eyes of male 5- to 6-wk-old C57BL6/J mice. A micropellet (0.35 × 0.35 mm) of sucrose and aluminum sulfate coated with Hydron polymer type NCC (Interferon Sciences, New Brunswick, NJ) containing 160 ng VEGF was implanted into each pocket. The pellet was positioned 0.6–0.8 mm from the corneal limbus. After implantation, erythromycin ophthalmic ointment was applied to each eye. For the inhibition study, mice that received corneal

implants containing VEGF were given SIM010603 daily by intragastric administration (i.g.). The eyes were examined by a slit-lamp biomicroscope on day 7 after pellet implantation. Vessel length and clock hours of circumferential neovascularization were measured. The neovascular area was calculated using the formula: area (mm^2) = 0.2 × π × maximal vessel length (mm) clock hours of neovascularization.

Tumor models

Exponentially growing cells were trypsinized and resuspended in sterile PBS and inoculated subcutaneously (s.c.) into the right flank of mice (T241-VEGF-A, MDA-MB-435, LLC-SW44, C57BL/6 mice; NCI-H460, BALB/c mice). Animals bearing tumors of a definite size were randomly divided into different groups receiving either vehicle (carboxy methyl cellulose) or SIM010603 (diluted in vehicle), dosed by oral gavage. Animal body weight and tumor measurements were obtained on scheduled days. Tumor volume (mm^3) was measured with Vernier calipers and calculated using the formula: length (mm) × width (mm) × width (mm) × 0.5. Percent growth inhibition of an individual tumor was calculated using the following formula: % growth inhibition = $(1 - [(T_L\_T_1)/(C_L\_C_1)] \times 100\%)$, where T_L and C_L are the treated and control tumor volumes on the last day, and T1 and C1 are treated and control tumor volumes on day 1. For all tumor growth inhibition experiments, 6–8 mice per dose group were used.

Whole-mount staining and immunofluorescent staining

Paraffin-embedded tumor tissues were sectioned at 20 μm thickness and fixed in 3% PFA (paraformaldehyde) overnight followed by treatment with proteinase K (20 μg/ml). Immunofluorescent staining was performed according to standard immunohistochemical procedures. Briefly, after 3 washes in PBS, specimens were incubated for 30 min in a blocking solution containing 4% nonimmune goat serum (Vector Laboratories) in PBS followed by incubation with primary antibodies for 2 h at room temperature. After 3 rigorous washes with PBS, tissues were incubated for 1 h at room temperature with secondary antibodies. Rat anti-mouse CD31 antibodies (BD-Pharmingen) were used as primary antibodies, and goat anti-rat Alexa Fluor 555-conjugated antibodies (Invitrogen) or goat anti-rat Alexa Fluor 647-conjugated antibodies (Invitrogen) were used as secondary antibodies. Additionally, a rabbit anti-mouse NG2 primary antibody (Chemicon International) and a goat anti-rabbit IgG Cy5-conjugated antibody (Invitrogen) were used as secondary antibodies. Sections were mounted on glass slides with Vectashield mounting medium (Vector Laboratories). Positive signals were photographed under a fluorescent microscope (Zeiss Confocal LSM510 Microscope). Quantitative analyses were obtained from at least 3 sections of 3 different animals. Digital images were processed in Adobe Photoshop CS.

Statistical analysis

Statistical analyses of in vitro and in vivo results were performed using the standard 2-tailed Student's t test in Microsoft Excel. $P < 0.05$ and $P < 0.01$ were deemed significant and extremely significant, respectively.

Results

Kinase assays

SIM010603 was tested against a total of 32 kinases in biochemical assays and was found to exhibit a high degree of selectivity for its target RTKs. SIM010603 inhibited activity of Kit, VEGFR, PDGFR-β, RET, and FLT3 with IC_{50} values ranging from 5.0 to 68.1 nmol/l (Table 1). Nontarget tyrosine kinases exhibited IC_{50} values in the range of ~500 to >10,000 nmol/l, so selectivity was generally in the range of ~150- to- 2,000-fold for target RTKs over other kinases evaluated (Supplementary information).

Activity of SIM010603 in cellular receptor phosphorylation assays

The potency of SIM010603 against tyrosine kinase enzyme preparations was reflected in receptor-mediated responses to $VEGF_{165}$ and PDGF-BB at the cellular level (Table 2). SIM010603 reduced $VEGF_{165}$-induced phosphorylation of VEGFR-2 in HUVECs and PDGF-BB-induced phosphorylation of PDGFR-β in NIH-3T3 cells in

Table 1 Kinases inhibitory activity profiles of SIM010603

Kinase	IC_{50} (nmol/l)
VEGFR-2	5.0
KIT	10.5
VEGF-R3	11.9
PDGFR-β	14.0
RET	68.1
FLT3	20.8
EGFR	>10,000
Src	>10,000
cMet	>10,000

Table 2 Inhibition of SIM010603 on cellular receptor phosphorylation

Cell	Receptor	Ligand	IC_{50} (nmol/l)
HUVEC	VEGFR-2	VEGF	24
NIH-3T3	PDGFR-β	PDGF-BB	68

a dose-dependent manner (IC_{50} = 24 nmol/l and 68 nmol/l, respectively).

Inhibition activity of SIM010603 on cell proliferation

Receptor phosphorylation in the VEGF pathway is an important mitogenic signal for endothelial cells [20]. As expected, SIM010603 inhibited $VEGF_{165}$-stimulated HUVECs proliferation and PDGF-BB-stimulated NIH-3T3 proliferation (IC_{50} = 53 nmol/l and 142 nmol/l, respectively). In contrast, with a panel of tumor cells grown in serum-containing media (Table 3), SIM010603 had only weak activity (IC_{50} > 1 μmol/l) against cells whose proliferation is not driven by a VEGF or PDGF tyrosine kinase. Anti-proliferative effects in these cellular assays are observed at >tenfold higher SIM010603 concentrations than in the VEGF-stimulated HUVEC assay.

Inhibition activity of SIM010603 on cell chemotaxis

SIM010603 inhibited VEGF-induced PAE-KDR cells chemotaxis in a dose-dependent manner (Fig. 2).

Corneal angiogenesis

We chose the mouse corneal angiogenesis model to study the effect of SIM010603 on angiogenesis because the cornea remains avascular under physiological conditions.

The angiogenic response stimulated by $VEGF_{165}$ was intense, with a high density of capillary sprouts.

Table 3 Inhibition of SIM010603 on cell proliferation

Cell	Growth factor*	IC_{50} (nmol/l)
HUVEC	VEGF	53
NIH-3T3	PDGF-BB	142
NIC-H460	FBS	6,150
T241-VEGF-A	FBS	>1,000
MDA-MB-435	FBS	>1,000
HT-29	FBS	1,200
A549	FBS	>1,000
BXPC-3	FBS	520
HepG2	FBS	7,270

Cells were incubated with SIM010603 for 72 h

* VEGF, 40 ng/ml; PDGF-BB, 30 ng/ml; FBS, 10% fetal bovine serum

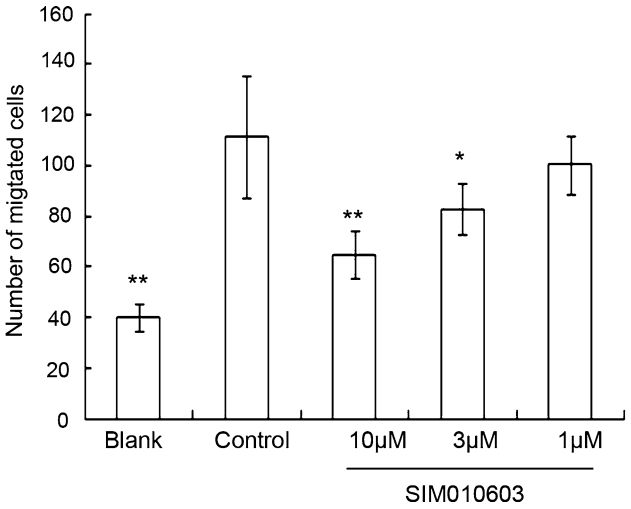

Fig. 2 Effect of SIM010603 on VEGF-induced PAE/VEGFR-2 chemotaxis. HUVECs were treated with SIM010603 as indicated in the upper chamber. After incubation for 4 h, the invasive cells were stained with Giemsa solution and counted under microscopy (×32). The data were presented as mean (SE). VEGF: 40 ng/ml; $^{**}P < 0.01$, $^{*}P < 0.05$ versus control, n = 4–6, repeated twice

The animals treated with SIM010603 consistently showed markedly reduced angiogenesis relative to control mice. When given daily for 7 days, 60 mg/kg SIM010603 significantly ($P < 0.01$) decreased $VEGF_{165}$-induced increase in vessel density in the cornea (Fig. 3).

Tumor growth inhibition

Anti-tumor activity of SIM010603 was evaluated in xenograft models using tumor cell lines including murine fibrosarcoma known to express VEGF-A (T241-VEGF-A), Lewis lung carcinoma (LLC-SW44), breast carcinoma (MDA-MB-435), and human lung carcinoma (NCI-H460).

Based on our preliminary data on the safety of SIM010603 (data not shown), 80 mg/kg/d was the least fatal dose of SIM010603 in a number of subcutaneous tumor xenograft models. Therefore, we chose 60 mg/kg/d as the highest dose to test the anti-tumor activity of SIM010603 in mice bearing T241-VEGF-A, LC-SW44, MDA-MB-435, and NCI-H460 tumors.

SIM010603 showed a dose-dependent growth inhibition of all the tumor xenografts tested (Fig. 4), although the degree of inhibition varied among different models. T241-VEGF-A, LC-SW44, and NCI-H460 showed a modest inhibition of tumor growth with inhibition reaching 52.00–59.50% at 60 mg/kg dose. MDA-MB-435 also showed 36.00% inhibition of tumor growth in mice treatment with 60 mg/kg SIM010603 (Table 4).

At all doses where tumor growth was inhibited, there were no signs of morbidity or weight loss.

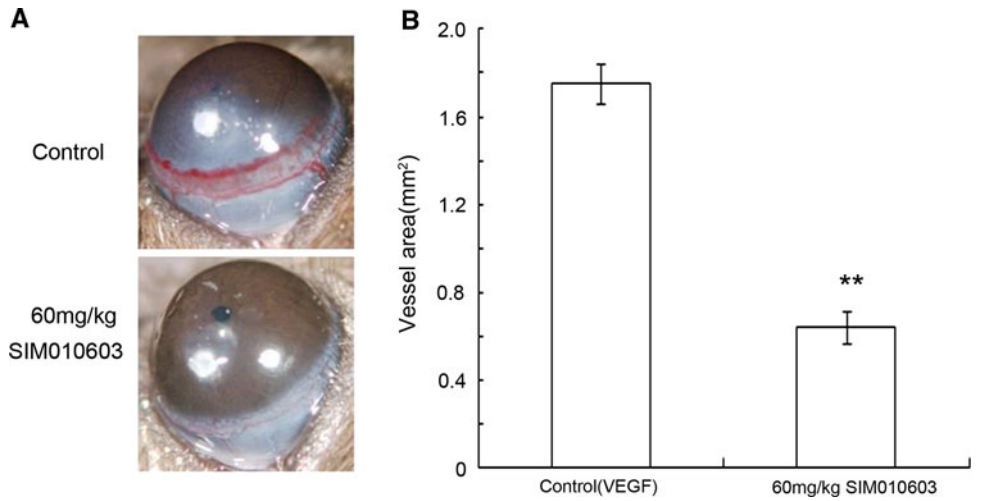

Fig. 3 Effect of SIM010603 on $VEGF_{165}$-induced corneal angiogenesis. VEGF-A with a slow-release polymer was implanted into the mouse cornea. The animals were given 60 mg/kg SIM010603 or vehicle daily by intragastric administration (i.g.) from postoperative days 1–7. **a** Biomicroscopic pictures of the newly formed vascular networks in the cornea. **b** Quantification of vessel area in VEGF-A-induced mouse cornea. The data are presented as mean (SE) ($n = 3$). $^{**}P < 0.01$, $^{*}P < 0.05$ versus control

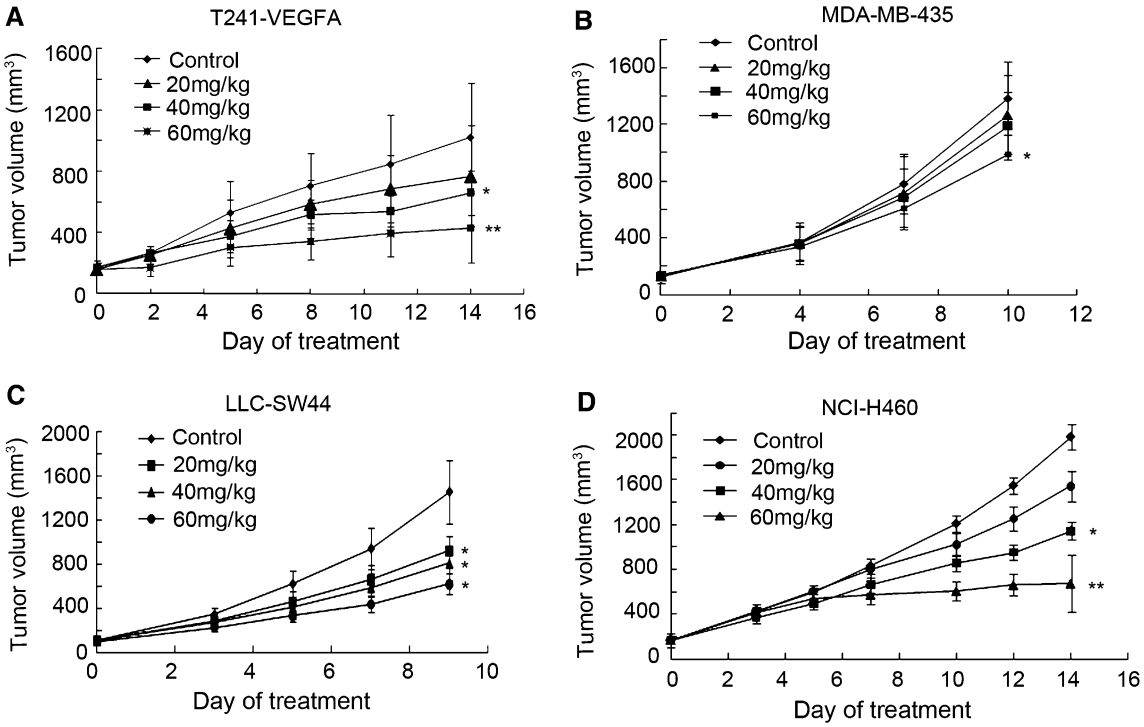

Fig. 4 Anti-tumor activity of SIM010603 on established **a** T241-VEGF-A, **b** MBA-MD-435, **c** LLS-SW44, and **d** NCI-H460 tumor xenografts in mice. Cells were inoculated s.c. Daily oral administration of SIM010603 at indicated dosages or vehicle was initiated when tumors reached a size of 100–200 mm^3 and continued through the end of the experiment. Tumor volume was measured on the indicated days, and the data are presented as mean (SE) ($n = 6$–8). $^{**}P < 0.01$, $^{*}P < 0.05$ versus control

Decreased MVD, pericyte recruitment, and pericyte encapsulation of vessels in tumor model

In addition to measuring changes in tumor volume, the anti-angiogenic activity of SIM010603 treatment in representative experiments was evaluated based on immunofluorescent analysis of tumors resected from treated and untreated animals. In T241-VEGF-A tumor model, the tumor vasculature consisted of disorganized, leaky, premature, torturous, and hemorrhagic blood vessels.

Table 4 Tumor growth inhibition of SIM010603 on established tumor xenografts

Tumor xenograft type	Dose (mg/kg)	Dosing regimen	% inhibition	*P* value
T241	20	p.o., daily, ×15d	30.00	>0.05
	40		41.60	<0.05
	60		59.50	<0.01
MDA-MB-435	20	p.o., daily, ×11d	10.20	>0.05
	40		16.10	>0.05
	60		36.00	<0.05
LLC-SW44	20	p.o., daily, ×10d	32.10	<0.05
	40		38.00	<0.05
	60		52.00	<0.05
NCI-H460	20	p.o., daily, ×15d	28.00	>0.05
	40		36.73	<0.05
	60		54.00	<0.01

Tumors were established as s.c. xenografts. Number of cells implanted per animal: 1×10^6. Daily treatment with oral SIM010603 or vehicle was initiated at the indicated dosages when tumors reached the indicted sizes. Percentage of growth inhibition values relative to vehicle-treated controls is indicated

These changes in tumor vessels are related to the persistent excretion of VEGF-A by T241-VEGF-A cells [21–23]. Treatment with SIM010603 decreased MVD and normalized tumor vessels (Fig. 5). In MDA-MB-435 models, significant numbers of CD31-positive endothelial cells and NG2-positive pericytes were found in the tumor tissue. Following dosing with 60 mg/kg SIM010603, tumor MVD, recruitment of pericytes, and pericyte encapsulation of tumor vessels significantly decreased (Fig. 6). Finally, in LLC-SW44 models, significant numbers of CD31-positive endothelial cells and NG2-positive pericytes were found in the tumor tissue. Treatment of 20 mg/kg SIM010603 decreased tumor MVD and had no effect on the recruitment of pericytes. As a result, treatment of 20 mg/kg SIM010603 increased pericyte encapsulation of tumor vessels in the LLC-SW44 tumor model. Although significantly decreased tumor MVD and recruitment of pericytes were observed, treatment of mice with 60 mg/kg SIM010603 had no effect on the pericyte encapsulation of tumor vessels in the LLC-SW44 tumor model (Fig. 7).

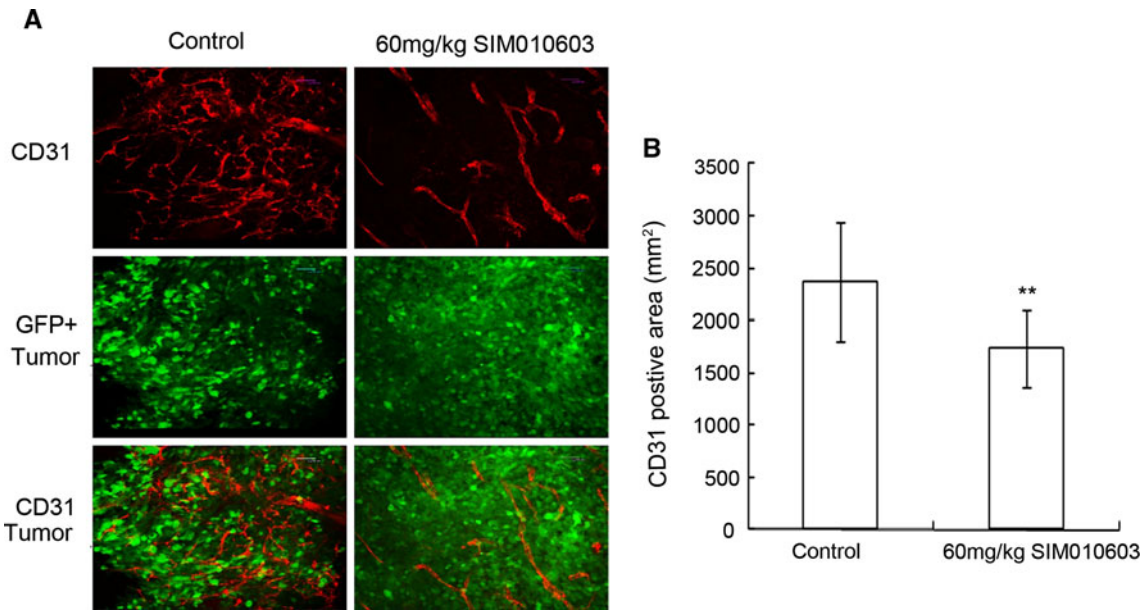

Fig. 5 Effect of SIM010603 on tumor vasculature in T241-VEGF-A xenograft tumor models. **a** VEGF-A-expressing tumor tissues were immunostained using anti-CD31 (*red*), and tumor cells expressed enhanced green fluorescence (*green*). *Scale bars*, 50 μm. **b** Quantification of microvessel density (CD31-postive area) in T241-VEGF-A tumors ($n = 4$–16 per group). The data are presented as mean (SE). $^{**}P < 0.01$, $^{*}P < 0.05$ versus control

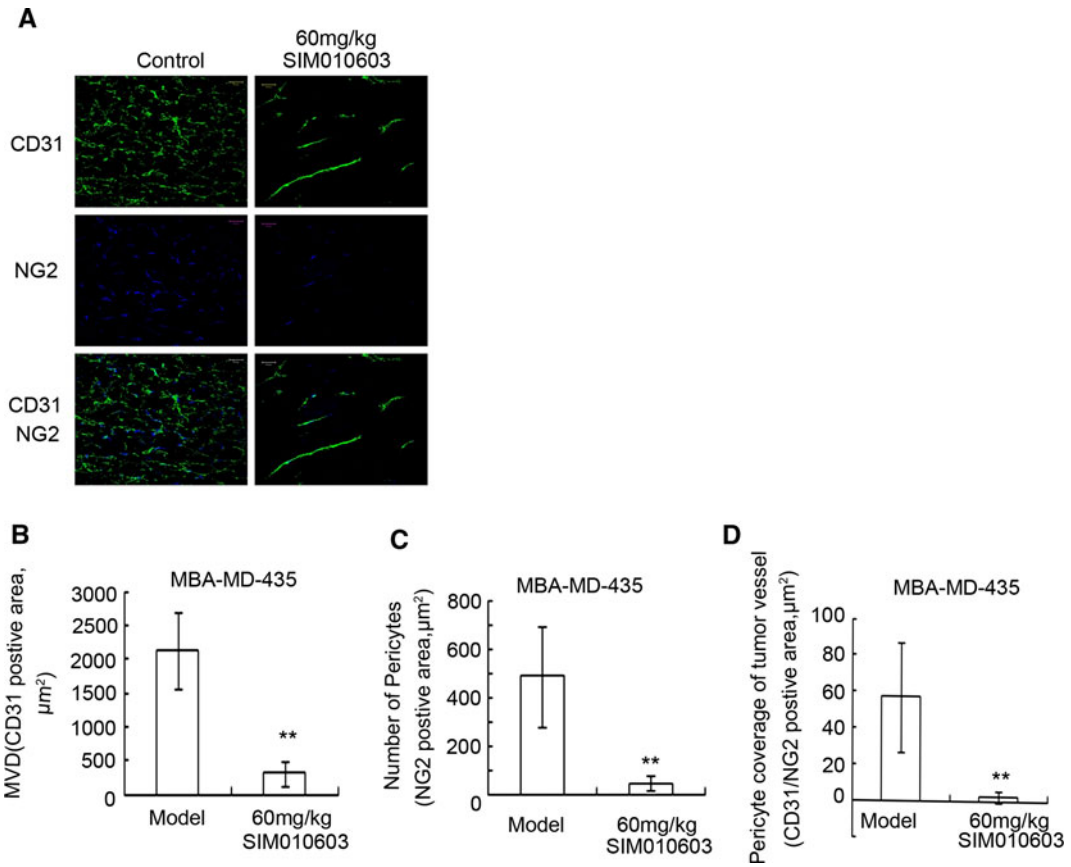

Fig. 6 Effect of SIM010603 on tumor vasculature, recruitment of pericytes, and pericyte encapsulation of tumor vessels in MDA-MB-435 xenograft tumor models. **a** Tumor tissues were double immunostained using anti-CD31 (*green*) and anti-NG2 (*blue*). *Scale bars*, 50 μm. **b–d** Quantification of microvessel density (CD31-postive area), recruitment of pericytes (NG2-postive area), and pericyte encapsulation of tumor vessels (percentage of CD31/NG2) in MDA-MB-435 tumor vasculature ($n = 10$–12 per group). The data are presented as mean (SE). $^{**}P < 0.01$, $^{*}P < 0.05$ versus control

Discussion

Cancer chemotherapy has been one of the major medical advances in the last few decades. However, the drugs used for this therapy have a narrow therapeutic index, and the responses produced are often only palliative as well as unpredictable. In contrast, targeted therapy, which has been introduced in recent years, is directed against cancer-specific molecules and signaling pathways and thus has more limited nonspecific toxicities.

RTK, such as VEGFR, DGFR, KIT, and FLT3, are expressed in malignant tissues and act in concert, playing diverse and major roles in angiogenesis, tumor growth, and metastasis. With the exception of a few malignancies, seemingly driven by a single genetic mutation in a signaling protein, most tumors are the product of multiple mutations in multiple aberrant signaling pathways. Consequently, simultaneous targeted inhibition of multiple signaling pathways could be more effective than inhibiting a single pathway in cancer therapies. Such a multi-targeted strategy has been validated in a number of preclinical and clinical studies using RTK inhibitors with broad target selectivity.

Compound containing an extended side chain at the C-3 position of the indolin-2-one has been identified to exhibit high potency and selectivity to inhibit PDGFRs and VEGFRs [24]. To improve the anti-tumor properties and optimize the pharmaceutical properties of 3-substituted indolin-2-ones, a number of different basic and weakly basic analogues were designed and synthesized. For example, sunitinib (SU11248; SUTENT; Pfizer, Inc., New York, NY) [25, 26], which was approved by the Food and Drug Administration for the treatment of advanced renal cell carcinoma and for the treatment of gastrointestinal stromal tumor after disease progression on, or intolerance to, imatinib mesylate therapy [27], is a potent inhibitor of receptor tyrosine kinases of VEGF, PDGFR, KIT, and FLT3. The mechanism of their receptor tyrosine kinase inhibition is through binding to the ATP-binding site of the intracellular kinase domain [28, 29].

By modifying the 3-substituted indolin-2-ones, we have identified a novel and orally active anti-tumor

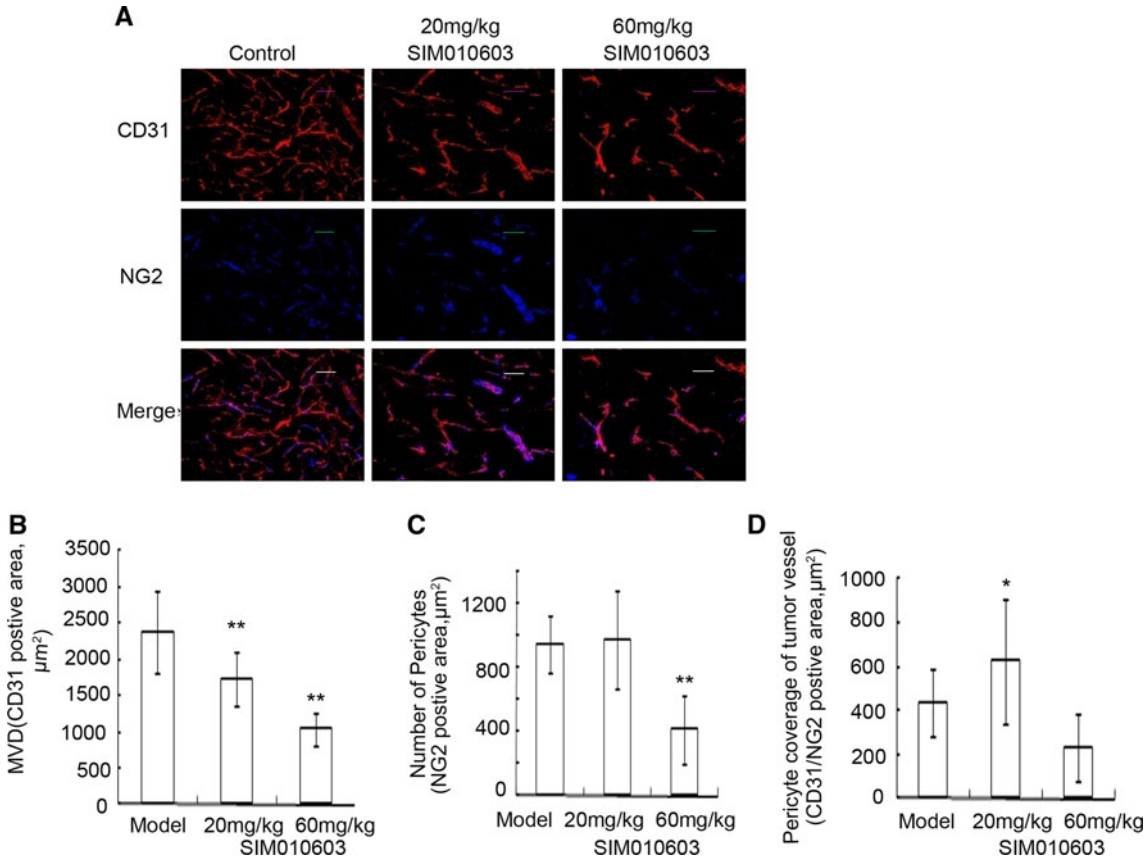

Fig. 7 Effects of SIM010603 on tumor vasculatures, recruitment of pericytes, and pericyte encapsulation of tumor vessels in LLC-SW44 xenograft tumor models. **a** Tumor tissues were double immunostained using anti-CD31 (*red*) and anti-NG2 (*blue*). *Scale bars*, 50 μm. **b–d** Quantification of microvessel density (CD31-postive area), recruitment of pericytes (NG2-postive area), and pericyte encapsulation of tumor vessels (percentage of CD31/NG2) in MDA-MB-435 tumor vasculature ($n = 10$–12 per group). The data are presented as mean (SE). $^{**}P < 0.01$, $^{*}P < 0.05$ versus control

agent—SIM010603. SIM010603 is similar in terms of structure and target profile to sunitinb. Like sunitinb, SIM010603 selectively inhibits multiple split kinase domain RTKs, including VEGFRs, PDGFR-β, KIT, and FLT3. Consistent with the putative mode of action defined using isolated enzyme preparations, SIM010603 showed an ability to inhibit $VEGF_{165}$-, PDGF-BB-stimulated receptor phosphorylation in intact cells.

SIM010603 exhibited efficacy in a broad spectrum of xenograft tumor growth models. Although regressions were not observed, all models showed growth inhibition and the tumor growth inhibition was dose responsive. There were no signs of morbidity or weight loss at any efficacious dose in the tumor growth inhibition studies, suggesting that SIM010603 is well tolerated at efficacious doses. Moreover, SIM010603 showed anti-tumor effects similar to SU11248.

Most of the tumor cell lines used for the efficacy studies reported here do not express RTKs targeted by SIM010603. Thus, it is likely that the anti-tumor activity of SIM010603 described here is related to the anti-angiogenic activity of SIM010603. To test this, we also determined the anti-angiogenic property of SIM010603.

In cellular assays, SIM010603 had the ability to potently inhibit $VEGF_{165}$-induced HUVECs proliferation and migration. The anti-angiogenic effect of SIM010603 in VEGF-A-stimulated corneal angiogenesis and xenograft tumor growth models also provided evidence of its anti-angiogenic properties.

VEGF and PDGF play an important role in tumor angiogenesis. VEGF promotes endothelial cell (EC) invasion and proliferation to form vessels through VEGFR on EC [30], and PDGFR promotes pericyte recruitment and encapsulation of tumor vessels to form thicker, more stable vessels [31–34]. To understand the effects of VEGFR-2 plus PDGFR-β targeting of SIM010603 on tumor blood vessel, we studied the pericyte–endothelial cell interaction in SIM010603-treated tumors. SIM010603 decreased MVD, pericyte recruitment in these tumor models. These results provide evidence of the contribution of SIM010603-mediated VEGFR and PDGFR inhibition on the anti-angiogenic activity of SIM010603.

Many preclinical studies have indicated that greater anti-angiogenic activity can be achieved by dual inhibition of VEGFR and PDGFR compared with selective inhibition of VEGFR or PDGFR alone [18, 35]. The simultaneous inhibition of VEGFR and PDGFR (which mediate tumor progression by multiple mechanisms) by SIM010603 might result in greater anti-tumor efficacy than more selective agents.

In summary, SIM010603 had a broad RTK inhibition spectrum and exhibited good anti-angiogenic and anti-tumor activities. In tumor models, SIM010603 not only decreased the tumor MVD, but also reduced the pericyte recruitment and pericyte encapsulation of tumor vessels. These preclinical characteristics of SIM010603 suggest that this molecule may offer advantages in cancer therapy and may be a new and promising agent for cancer therapy.

Acknowledgments This work was supported by grants from Mega-projects of Science Research for the 11th Five-Year Plan: Preclinical study of molecular-target drug SIM010603 (No. 2009ZX09102-002).

References

1. Gatzemeier U, Blumenschein G, Fosella F, Simantov R, Elting J, Bigwood D et al (2006) Phase II trial of single-agent sorafenib in patients with advanced non-small cell lung carcinoma. J Clin Oncol 24(Suppl):364s
2. Hurwitz H, Fehrenbacher L, Novotny W, Cripe L, McGuire W, Wertheim M et al (2007) Integrated report of the phase 2 experience with XL999 administered IV to patients (pts) with NSCLC, renal cell CA (RCC), metastatic colorectal CA (CRC), recurrent ovarian CA, acute myelogenousleuk aemia (AML), and multiple myeloma (MM). J Clin Oncol 25(Suppl):160s
3. Ross RW, Stein M, Sarantopoulos J, Eisenberg P, Logan T, Srinivas S et al (2007) A phase II study of the c-Met RTK inhibitor XL880 in patients (pts) with papillary renal-cell carcinoma (PRC). J Clin Oncol 25(Suppl):658s
4. Tibes R, Trent J, Kurzrock R (2005) Tyrosine kinase inhibitors and the dawn of molecular cancer therapeutics. Ann Rev Pharmacol Toxicol 45:357–384
5. Blume-Jensen P, Hunter T (2001) Oncogenic kinase signalling. Nature 411:355–365
6. Sawyers CL (1999) Chronic myeloid leukemia. N Engl J Med 340:1330–1340
7. Shah NP, Nicoll JM, Nagar B, Gorre ME, Paquette RL, Kuriyan J et al (2002) Multiple BCR-ABL kinase domain mutations confer polyclonal resistance to the tyrosine kinase inhibitor imatinib (STI571) in chronic phase and blast crisis chronic myeloid leukemia. Cancer Cell 2:117–125
8. Pao W, Miller V, Zakowski M, Doherty J, Politi K, Sarkaria I et al (2004) EGF receptor gene mutations are common in lung cancers from "never smokers" and are associated with sensitivity of tumors to gefitinib and erlotinib. Proc Natl Acad Sci 101:13306–13311
9. Baselga J, Arteaga CL (2005) Critical update and emerging trends in epidermal growth factor receptor targeting in cancer. J Clin Oncol 23:2445–2459
10. Paez JG, Janne PA, Lee JC, Tracy S, Greulich H, Gabriel S et al (2004) EGFR mutations in lung cancer: correlation with clinical response to gefitinib therapy. Science 304:1497–1500
11. Petrelli A, Giordano S (2008) From single- to multi-target drugs in cancer therapy: when aspecificity becomes an advantage. Curr Med Chem 15(5):422–432
12. Ocanal A, Serrano R, Calero R, Pandiella A (2009) Novel tyrosine kinase inhibitors in the treatment of cancer. Curr Drug Targets 10(6):575–576
13. Cao R, Xue Y, Hedlund EM, Zhong Zh, Tritsaris K, Tondelli B, Lucchini F et al (2010) VEGFR1—mediated pericyte ablation links VEGF and PlGF to cancer-associated retinopathy. Proc Natl Acad Sci 107:856–861
14. Hedlund EM, Hosaka K, Zhong ZH, Cao R, Cao Y (2009) Malignant cell-derived PlGF promotes normalization and remodeling of the tumor vasculature. Proc Natl Acad Sci 106:17505–17510
15. Sanghera J, Li R, Yan J (2009) Comparison of the luminescent ADP-Glo assay to a standard radiometric assay for measurement of protein kinase activity. Assay Drug Dev Technol 7(6): 615–622
16. Roberts WG, Whalen PM, Soderstrom E, Moraski G, Lyssikatos JP, Wang HF et al (2005) Antiangiogenic and antitumor activity of a selective PDGFR tyrosine kinase inhibitor, CP-673, 451. Cancer Res 65(3):957–966
17. Cao Y, Linden P, Farnebo J, Cao R, Eriksson A, Kumar V et al (1998) Vascular endothelial growth factor C induces angiogenesis in vivo. Proc Natl Acad Sci 95:14389–14394
18. Labrecque L, Lamy S, Chapus A, Mihoubi S, Durocher Y, Cass B et al (2005) Combined inhibition of PDGF and VEGF receptors by ellagic acid, a dietary-derived phenolic compound. Carcinogenesis 26:821–826
19. Cao R, Brakenhielm E, Wahlestedt C, Thyberg J, Cao Y (2001) Leptin induces vascular permeability and synergistically stimulates angiogenesis with FGF-2 and VEGF. Proc Natl Acad Sci 98:6390–6395
20. Leung DW, Cachianes G, Kuang WJ, Goeddel DV, Ferrara N (1989) Vascular endothelial growth factor is a secreted angiogenic mitogen. Science 246:1306–1309
21. Carmeliet P (2005) Angiogenesis in life, disease and medicine. Nature 438:932–936
22. Chen F, Xue Y, Cao Y, Han B (2009) Cancer-associated systemic syndrome (CASS): the mechanism of VEGF in tumor-bearing mice. Chin J Lung Cancer 12(4):30–35
23. Xue Y, Religa P, Cao R, Hansen AJ, Lucchini F, Jones B et al (2008) Anti-VEGF agents confer survival advantages to tumor-bearing mice by improving cancer-associated systemic syndrome. Proc Natl Acad Sci 105(47):18513–18518
24. Sun L, Tran N, Tang F, App H, Hirth P, McMahon G et al (1998) Synthesis and biological evaluations of 3-substituted indolin-2-ones: a novel class of tyrosine kinase inhibitors that exhibit selectivity toward particular receptor tyrosine kinases. J Med Chem 41(14):2588–2603
25. Mendel DB, Laird AD, Xin X, Louie SG, Christensen JG, Schreck RE et al (2003) In vivo antitumor activity of SU11248, a novel tyrosine kinase inhibitor targeting vascular endothelial growth factor and platelet-derived growth factor receptors: determination of a pharmacokinetic/pharmacodynamic relationship. Clin Cancer Res 9:327–337
26. O'Farrell AM, Abrams TJ, Yuen HA, Ngai TJ, Louie SG, Yee KWH et al (2003) SU11248 is a novel FLT3 tyrosine kinase inhibitor with potent activity in vitro and in vivo. Blood 101:3597–3605
27. SUTENT (sunitinibmalate) prescribing information (2006) Pfizer. Inc., New York
28. Mohammadi M, McMahon G, Sun L, Tang C, Hirth P, Yeh BK, Hubbard SR et al (1997) Structures of the tyrosine kinase domain of fibroblast growth factor receptor in complex with inhibitors. Science 276:955–960

29. Sun L, Tran N, Liang C, Tang F, Rice A, Schreck R et al (1999) Design, synthesis, and evaluations of substituted 3-[(3- or 4-carboxyethylpyrrol-2-yl)methylidenyl]indolin-2-ones as inhibitors of VEGF, FGF, and PDGF receptor tyrosine kinases. J Med Chem 42(5):5120–5130
30. Ferrara N, Gerber HP, LeCouter J (2003) The biology of VEGF and its receptors. Nat Med 9:669–676
31. Andrae J, Gallini R, Betsholtz C (2008) Role of platelet-derived growth factors in physiology and medicine. Genes Dev 22:1276–1312
32. Zhang XH, Lin LP, Ding J (2006) Platelet-derived growth factor receptor and cancer. Chin Bull Life Sci 18(3):220–226
33. Tallquist M, Kazlauskas A (2004) PDGF signaling in cells and mice. Cytokine Growth Factor Rev 15(4):205–213
34. Vincent L, Rafii S (2004) Vascular frontiers without borders: multifaceted roles of platelet-derived growth factor (PDGF) in supporting postnatal angiogenesis and lymphangiogenesis. Cancer Cell 6:307–309
35. Yao VJ, Sennino B, Davis RB et al (2006) Combined anti-VEGFR and anti-PDGFR actions of sunitinib on blood vessels in preclinical tumor models. Presented at the 18th EORTC–NCI–AACR symposium, Prague, Czech Republic, 7–10 November 2006